ChemComm

COMMUNICATION

View Article Online
View Journal

Check for updates

Cite this: DOI: 10.1039/d5cc01565k

Received 19th March 2025,
Accepted 11th April 2025

DOI: 10.1039/d5cc01565k

rsc.li/chemcomm

Published on 17 April 2025. Downloaded by Shanghai Normal University on 4/30/2025 1:45:42 AM.

A novel CRISPR–Cas12a-based fluorescence anisotropy method with a high signal-to-background ratio for sensitive biosensing†

Yu Qin,‡[a] Jia Li Xie,‡[a] Kai Mao,[a] Yuan Fang Li,[a] Cheng Zhi Huang,[b] Hong Yan Zou*[b] and Shu Jun Zhen*[a]

Here, a CRISPR–Cas12a system with high trans-cleavage ability integrating a DNA nanochain formed by DNA tetrahedrons with a large molecular mass was employed to enhance the signal-to-background ratio of the fluorescence anisotropy method for achieving sensitive detection of hepatitis B virus DNA.

Fluorescence anisotropy (FA) is a phenomenon where fluorescent molecules have unequal emission intensities along different polarization axes.[1,2] As a ratiometric technique, the FA assay is less sensitive to photobleaching and small signal fluctuations compared to traditional fluorescence-based methods.[3–7] In addition, FA analysis is a simple, homogeneous technique that involves directly mixing the probe and target.[8–10] These advantages broaden its applications, and the FA method has been utilized for the detection of numerous biomolecules based on the principle that the strength of the polarization signal of the fluorophore is inversely proportional to the rate of its molecular rotation.[11–13]

Traditionally, nucleic acid probes (NAPs) are frequently designed as recognition units in FA analyses.[14–18] To generate an FA signal response, fluorescent dyes are usually linked to NAPs. However, due to the large molecular mass of NAPs, it has a high FA value (r). In other words, the background signal is high, so the change of r after adding the target is not obvious, resulting in poor sensitivity. Although many FA signal amplification methods have been reported, they only focus on enhancing the FA response with a series of molecular-mass-amplifying materials.[19] For example, our research group previously reported the use of graphene oxide (GO),[20] submicro-hydrogels[21] and a DNA nanosheet (DNS)[22] with large molecular masses as FA amplifiers to detect biomolecules. Zhang *et al.* proposed utilizing antibodies to enhance FA signals to detect aflatoxin B1 and adenosine.[8] However, an ideal FA method should not only have strong signals but also low background noise.

Recently, the clustered regularly spaced short palindromic repeats (CRISPR) and associated proteins (Cas) system (CRISPR/Cas) was discovered in bacteria and archaea and has been widely applied in the bioanalysis and diagnostic fields.[23–25] Cas12a, a typical class 2 type V Cas nuclease binding to the CRISPR RNA transfer (crRNA), can realize nonspecific trans-cleavage of single-stranded DNA (ssDNA) to small fragments after recognizing the DNA targets.[26–30] Thus, many short-stranded fluorophore-modified nucleic acids with low masses and volumes can be obtained. Due to the aforementioned benefits, the CRISPR–Cas12a system has been proved to have an excellent ability to decrease the background of FA detections, as shown by our group.[31–33]

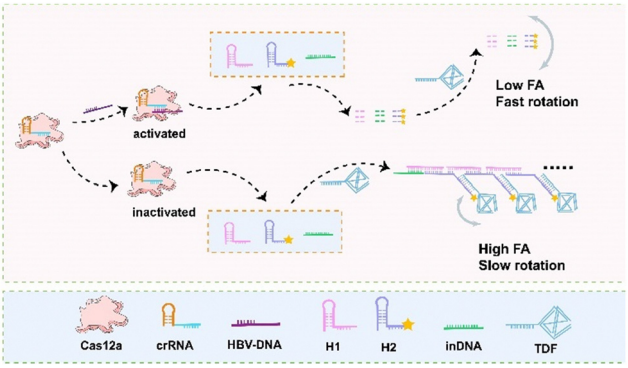
In this work, to further improve the sensitivity of FA detection, a novel FA method with a high signal-to-background ratio (SBR) was designed for achieving sensitive detection of hepatitis B virus DNA (HBV-DNA), a major pathogen of viral hepatitis, cirrhosis, and liver cancer.[34–37] Here, a DNA nanochain formed by the assembly of a hybridization chain reaction (HCR) product with DNA tetrahedrons (TDFs) was designed as molecular mass amplification material to enhance FA signals. At the same time, the background signal was reduced by utilizing the trans-cleavage property of CRISPR–Cas12a. In the absence of HBV-DNA, the CRISPR–Cas12a system was inactivated. Then, the HCR was started to form a long dsDNA nanostructure, which can assemble with many TDFs to form the DNA nanochain structure to enhance the FA because of the remarkably enhanced molecular mass. In contrast, when HBV-DNA was present, the CRISPR–Cas12a system was activated, and the carboxytetramethyl-rhodamine (TAMRA)-labelled nucleic acids were cut into small pieces with much lower molecular mass, resulting in significantly decreased r. Integrating the CRISPR–Cas12a system with the DNA nanochain

[a] College of Chemistry and Chemical Engineering, Southwest University, 400715, Chongqing, P. R. China. E-mail: zsj@swu.edu.cn
[b] Key Laboratory of Biomedical Analytics, Chongqing Science and Technology Bureau, College of Pharmaceutical Sciences, Southwest University, 400715, Chongqing, P. R. China. E-mail: zhy2013@swu.edu.cn

† Electronic supplementary information (ESI) available. See DOI: https://doi.org/10.1039/d5cc01565k

‡ These authors contributed equally to this work.

Published on 17 April 2025. Downloaded by Shanghai Normal University on 4/30/2025 1:45:42 AM.



Scheme 1 Illustration of working principle of HBV-DNA detection using the CRISPR–Cas12a system and DNA-nanochain-induced FA amplification assay.

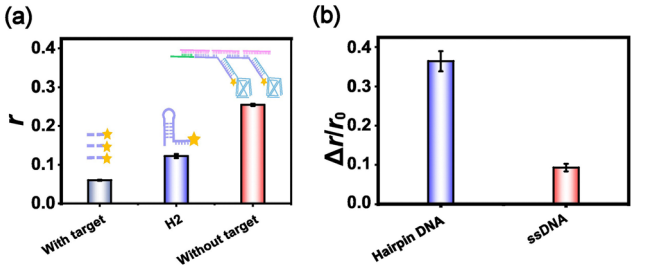


Fig. 1 Feasibility analysis of the proposed strategy. (a) Fluorescence anisotropy (r) values of H2 with and without target HBV-DNA. Each value shown resulted from triplicate measurements (with error bars indicating standard deviation). Concentrations: HBV-DNA, 25 nM; Cas12a, 20 nM; crRNA, 20 nM; H1, 50 nM; H2, 50 nM; inDNA, 50 nM; TDF, 50 nM. (b) The $\Delta r/r_0$ of hairpin DNA and ssDNA incubated with Cas12a–crRNA after the addition of HBV-DNA with the same concentrations. Each value shown resulted from triplicate measurements (with error bars indicating standard deviation). Concentrations: HBV-DNA, 0.7 nM; Cas12a, 20 nM; crRNA, 20 nM; Harpin DNA, 50 nM; ssDNA, 50 nM.

improved the SBR and greatly enhanced the sensitivity for HBV-DNA detection.

The principle of HBV-DNA detection is illustrated in Scheme 1. The Cas12a–crRNA complex was first generated by combining Cas12a with crRNA. In the absence of the target HBV-DNA, the CRISPR–Cas12a system failed to be activated. In this way, H1, TAMRA-modified H2, and inDNA remained intact. In this situation, inDNA initiated the HCR circuit, forming a long double-stranded DNA structure that assembled with numerous TDFs into a DNA nanochain. Thus, the FA signal of TAMRA on H2 was greatly enhanced because of the large molecular mass of the DNA nanochain. In the presence of target HBV-DNA, the protospacer adjacent motif (PAM) of the HBV-DNA domain can recognize crRNA, triggering the nonspecific trans-cleavage ability of the CRISPR–Cas12a system to cut H1, H2, and inDNA into small pieces, resulting in an extremely weak FA signal. Therefore, HBV-DNA could be sensitively detected through the markedly weakened background signal and obviously enhanced FA response.

To verify the successful assembly of HCR products and TDFs, 12% native polyacrylamide gel electrophoresis (PAGE) was deployed. As shown in Fig. S1a (ESI†), when all four DNA components (S1, S2, S3, S4) of TDF were present, the migration rate of the bands was the lowest, indicating that TDF was successfully formed. Meanwhile, it could be seen from Fig. S1b (ESI†) that in the absence of inDNA, whether H1 and H2 were present alone or together, they appeared as their own separate bands, indicating that the two hairpin DNAs could stably coexist in solution. After the addition of inDNA, a series of strips with migration rates lower than those of H1 and H2 strips were observed, attributed to HCR having produced long double-stranded structures. The atomic force microscope (AFM) images confirmed the successful formation of HCR products and DNA nanochain structures (Fig. S1c and d, ESI†).

Then, the trans-cleavage capability of CRISPR–Cas12a was studied. The gel images (Fig. S2a, ESI†) showed that when the Cas12a–crRNA complex was co-incubated with target, the H2 band almost disappeared. At the same time, the band position of the Cas12a–crRNA complex and that of the target did not change. Next, the ssDNA, modified with the 6-carboxyfluorescein (FAM) fluorescent dye on one end and black hole quencher (BHQ) on the other end, was used as the reporter. Because of the fluorescence resonance energy transfer (FRET) between FAM and BHQ, the fluorescence signal of FAM was low before the addition of HBV-DNA. In contrast, the addition of HBV-DNA into the Cas12a–crRNA complex significantly restored the fluorescence intensity of FAM (Fig. S2b, ESI†). These results confirmed that the CRISPR–Cas12a system could be activated when the target was added.

As shown in Fig. 1a, the H2 sample itself exhibited a high r value. With the addition of target, HBV-DNA hybridized with crRNA, triggering the trans-cleavage ability of CRISPR to cut H2 into small segments, resulting in much lower r values. In contrast, in the absence of target, the r value was enhanced greatly, due to the large volume and mass of the DNA nanochain. As expected, the CRISPR–Cas12a system effectively weakened the background signal, while the DNA nanochain enhanced the FA response. That is to say, our proposed method produced a very high SBR. Next, we compared the cutting efficiency of the CRISPR–Cas12a system on hairpin DNA with that on single-stranded DNA (ssDNA) with the same number of bases. In general, hairpin DNA, due to its self-complementarity, can form stable secondary structures; this structure enables it to exhibit a more rigid and predictable conformation, making it easier for CRISPR–Cas12a complexes to recognize and bind.[38] As depicted in Fig. 1b, in the current work, after adding HBV-DNA into the mixture of CRISPR–Cas12a and H2, a strong signal change $\Delta r/r_0$ ($\Delta r = r_0 - r$, with r_0 denoting the FA value in the absence of HBV-DNA, and r the FA value in the presence of HBV-DNA) was observed. In contrast, $\Delta r/r_0$ was significantly lower when HBV-DNA with the same concentration was added to a mixture of CRISPR–Cas12a and ssDNA, suggesting that the hairpin DNA was more readily cut by the CRISPR–Cas12a system than by ssDNA. Consequently, our strategy can be utilized for the sensitive detection of HBV-DNA.

Under the optimal experimental conditions (Fig. S3, ESI†), we measured the FA responses of HBV-DNA at different

 This journal is © The Royal Society of Chemistry 2025

Published on 17 April 2025. Downloaded by Shanghai Normal University on 4/30/2025 1:45:42 AM.

concentrations. As shown in Fig. 2a, $\Delta r/r_0$ exhibited a strong linear correlation with HBV-DNA concentration ranging from 10 pM to 1.2 nM and following the linear regression equation $\Delta r/r_0 = 0.587\,c + 0.134$ (correlation coefficient, $R^2 = 0.995$), with c denoting the concentration of HBV-DNA (nM). The limit of detection (LOD) was calculated to be 3.8 pM based on 3σ/slope. Thus, the combination of CRISPR–Cas12a and the DNA nanochain showed a high sensitivity toward the target HBV-DNA. Furthermore, a comparative study with other methods for detecting HBV-DNA was conducted. As shown in Table S2 (ESI†), our method was found to outperform others in terms of both detection limit and sensitivity. At the same time, we compared the sensitivity of our method with that of the reported FA methods for detecting nucleic acid targets. As illustrated in Table S3 (ESI†), our approach was found to display higher sensitivity for detecting nucleic acid targets. Furthermore, we investigated the FA sensor with only the CRISPR–Cas12a system (Fig. 2b) and only the nanochain (Fig. 2c). As shown in Fig. 2d, when only using the CRISPR–Cas12a system, there was a positive linear relationship between $\Delta r/r_0$ and the concentration of HBV-DNA in the range 0.1 to 1.1 nM. Furthermore, the LOD of this system was 30 pM. As shown in Fig. 2e, the linear range was 1 to 70 nM with an LOD of 420 pM when only the DNA nanochain was present. That is to say, adding the CRISPR–Cas12a system enhanced the detection sensitivity about 84 fold. However, when only using the nanochain to enhance the FA signal, the detection sensitivity was just 2 times higher than that without the nanochain. Collectively, the presence of the CRISPR–Cas12a system and DNA nanochain could indeed improve the sensitivity for detecting HBV-DNA and enhance the SBR of the detection of HBV-DNA.

Next, the selectivity of our proposed method was validated by studying 1-base–mismatched HBV (mis-1), 2-base-mismatched HBV (mis-2), 3-base-mismatched HBV (mis-3), and random sequences (rs). As illustrated in Fig. 3a, the $\Delta r/r_0$ signals of all these cases were much lower than that for HBV-DNA, indicating an excellent specificity of our method.

In general, hepatitis B virus is usually tested by measuring the amount of HBV-DNA in human serum. However, serum contains large numbers of ions, small molecules and proteins, which may interfere with the detection of HBV-DNA. Therefore, in the current work, the anti-interference ability of this strategy in a real matrix was investigated. The ratio of the concentration of the potentially interfering substance to that of HBV-DNA was set at 10 : 1. The results showed that the potentially interfering proteins had in fact little effect on the $\Delta r/r_0$ signal (Fig. 3b). Furthermore, after adding different metal ions and other small molecule substances to the HBV-DNA-containing solutions, the $\Delta r/r_0$ values were almost the same as that after the addition of only HBV-DNA. Therefore, our proposed approach demonstrated excellent anti-interference capability for the detection of HBV-DNA.

In actual clinical diagnosis, serum contains numerous substances that can interfere with target detection. To evaluate the accuracy of the proposed method in complex samples, a spike-recovery experiment was performed; specifically, recoveries of HBV-DNA spiked in human serum samples were examined. As listed in Table S4 (ESI†), the recovery rate of the FA signal ranged from 91.5% to 106.5%, with relative standard deviation (RSD) values of 0.03% to 0.06%. These results indicated the

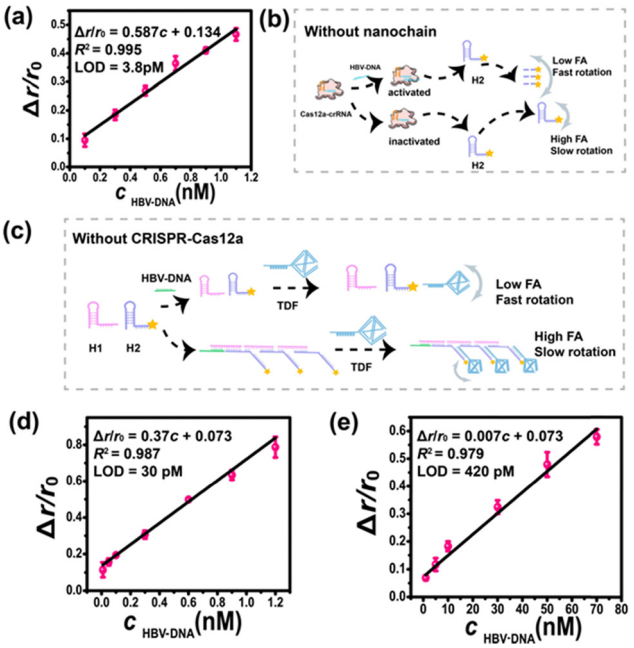


Fig. 2 Comparison of the sensitivities of different FA amplification strategies. (a) Plot showing a linear relationship between $\Delta r/r_0$ and HBV-DNA concentration with the double amplification effect of CRISPR–Cas12a and the DNA nanochain. (b) Schematic diagram of the strategy involving CRISPR–Cas12a-amplified FA. (c) Schematic diagram of the strategy involving DNA-nanochain-amplified FA. (d) Plot showing a linear relationship between $\Delta r/r_0$ and HBV-DNA concentration with the amplification effect of CRISPR–Cas12a. (e) Plot showing a linear relationship between $\Delta r/r_0$ and HBV-DNA concentration with the amplification effect of the DNA nanochain. Concentrations: Cas12a, 20 nM; crRNA, 20 nM; H1, 50 nM; H2, 50 nM; inDNA, 50 nM; TDF, 50 nM.

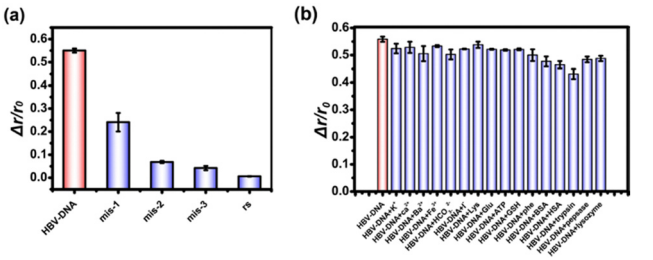


Fig. 3 (a) Selectivity of the proposed method. (b) Plot showing lack of interference of common proteins, ions and small molecules with the proposed method, ions and small molecules to the proposed method. Each value shown resulted from triplicate measurements (with error bars indicating standard deviation). Concentrations: HBV-DNA, 600 pM; Cas12a, 20 nM; crRNA, 20 nM; H1, 50 nM; H2, 50 nM; inDNA, 50 nM; TDF, 50 nM. K^+, Ca^{2+}, Ba^{2+}, Fe^{3+}, CO_3^{2-}, I^-, lysine (Lys), glutamate (Glu), adenosine triphosphate (ATP), glutathione (GSH), phenylalanine (Phe), bovine serum albumin (BSA), human serum albumin (HSA), trypsin, pepsase, lysozyme, 6 nM.

Published on 17 April 2025. Downloaded by Shanghai Normal University on 4/30/2025 1:45:42 AM.

good potential for this work in clinical detection and an expectation of its application in clinical practice.

In summary, a novel strategy was proposed for the sensitive detection of HBV-DNA, involving the use of CRISPR–Cas12a and a DNA nanochain to assist in amplifying FA signals. The activated CRISPR–Cas12a system could decrease the background signal significantly, while the long nanochain with many TDFs could significantly enhance the FA signal. Thus, combining the high collateral cleavage activity of the CRISPR–Cas12a system and the nanochain with its good FA amplification ability significantly improved the SBR for HBV-DNA detection. The sensitivity of our method was especially prominent in the FA analysis. As anticipated, the developed FA method was successfully applied in HBV-DNA detection with good sensitivity and accuracy, which has the potential to aid in clinical diagnosis.

Yu Qin: conceptualization, investigation, data and formal analysis, writing – original draft. Jia Li Xie: investigation, visualization, validation, data and formal analysis, writing – original draft. Kai Mao: validation, formal analysis. Cheng Zhi Huang: resources, supervision. Yuan Fang Li: writing – review and editing. Hong Yan Zou: methodology, writing – review and editing. Shu Jun Zhen: methodology, funding acquisition, writing – review and editing, supervision.

This work was supported by the National Natural Science Foundation of China (No. 22322409, 21974109).

Data availability

The data supporting this article have been included in the main article and as part of the ESI.†

Conflicts of interest

There are no conflicts to declare.

Notes and references

1 Q. Huang, B. Chen, J. Shen, L. Liu, J. Li, J. Shi, Q. Li, X. Zuo, L. Wang, C. Fan and J. Li, *J. Am. Chem. Soc.*, 2021, **143**, 10735–10742.
2 J. R. Lakowicz and B. R. Masters, *J. Biomed. Opt.*, 2008, **13**, 029901.
3 J. Chen, J. Liu, X. Chen and H. Qiu, *Chin. Chem. Lett.*, 2019, **30**, 1575–1580.
4 Y. L. Fan, Z. Y. Liu, Y. M. Zeng, L. Y. Huang, Z. Li, Z. L. Zhang, D. W. Pang and Z. Q. Tian, *Talanta*, 2021, **223**, 121721.
5 Y. Y. Fan, Z. L. Mou, M. Wang, J. Li, J. Zhang, F. Q. Dang and Z. Q. Zhang, *Anal. Chem.*, 2018, **90**, 13708–13713.
6 D. Zhang, R. Fu, Q. Zhao, H. Rong and H. Wang, *Anal. Chem.*, 2015, **87**, 4903–4909.
7 D. Zhang, J. Wang, Z. Tong, H. Ji and H. Qu, *Adv. Funct. Mater.*, 2021, **31**, 2106577.
8 Y. Li, H. Yu and Q. Zhao, *RSC Adv.*, 2022, **12**, 7464–7468.
9 P. Ma, H. Guo, N. Duan, X. Ma, L. Yue, Q. Gu and Z. Wang, *Talanta*, 2021, **230**, 122349.
10 B. Yang, X. B. Zhang, L. P. Kang, G. L. Shen, R. Q. Yu and W. Tan, *Anal. Chem.*, 2013, **85**, 11518–11523.
11 K. Chullipalliyalil, K. Elkassas, M. A. P. McAuliffe, S. Vucen and A. Crean, *Anal. Chem.*, 2023, **95**, 2774–2782.
12 X. Xiao and S. Zhen, *RSC Adv.*, 2022, **12**, 6364–6376.
13 Q. Zhu, H. Li and D. Xu, *RSC Adv.*, 2020, **10**, 17037–17044.
14 Y. Huang, S. Zhao, Z. F. Chen, Y. C. Liu and H. Liang, *Chem. Commun.*, 2011, **47**, 4763.
15 Y. Li and Q. Zhao, *Anal. Chem.*, 2019, **91**, 7379–7384.
16 X. Xiao, Y. F. Li, C. Z. Huang and S. J. Zhen, *Chem. Commun.*, 2015, **51**, 16080–16083.
17 S. J. Zhen, X. Xiao, C. H. Li and C. Z. Huang, *Anal. Chem.*, 2017, **89**, 8766–8771.
18 Z. Zhu, T. Schmidt, M. Mahrous, V. Guieu, S. Perrier, C. Ravelet and E. Peyrin, *Anal. Chim. Acta*, 2011, **707**, 191–196.
19 Y. Yu, Y. Liu, S. J. Zhen and C. Z. Huang, *Chem. Commun.*, 2013, **49**, 1942.
20 X. Xiao and S. J. Zhen, *RSC Adv.*, 2022, **12**, 6364–6376.
21 Y. X. Liu, T. J. Xie, C. H. Li, Q. C. Ye, L. L. Tian, Y. F. Li, C. Z. Huang and S. J. Zhen, *Anal. Chim. Acta*, 2021, **1154**, 338319.
22 Y. X. Liu, X. Xiao, C. H. Li, C. Men, Q. C. Ye, W. Y. Lv, Y. F. Li, C. Z. Huang and S. J. Zhen, *Talanta*, 2020, **211**, 120730.
23 M. Liang, Z. Li, W. Wang, J. Liu, L. Liu, G. Zhu, L. Karthik, M. Wang, K.-F. Wang, Z. Wang, J. Yu, Y. Shuai, J. Yu, L. Zhang, Z. Yang, C. Li, Q. Zhang, T. Shi, L. Zhou, F. Xie, H. Dai, X. Liu, J. Zhang, G. Liu, Y. Zhuo, B. Zhang, C. Liu, S. Li, X. Xia, Y. Tong, Y. Liu, G. Alterovitz, G.-Y. Tan and L.-X. Zhang, *Nat. Commun.*, 2019, **10**, 3672.
24 Q. Du, H. Zhang, Y. Bi, H. Wang, X. Zhou, P. Shi, S. Lv and S. Bi, *Anal. Chem.*, 2025, **97**, 4049–4056.
25 X. Ma, Y. Zhang, X. Qiao, Y. Yuan, Q. Sheng and T. Yue, *Anal. Chem.*, 2023, **95**, 11723–11731.
26 J. De Dieu Habimana, O. Mukama, O. B. Amissah, Y. Sun, E. Karangwa, Y. Liu, S. Mugisha, N. Cheng, L. Wang, J. Chen, S. Deng, R. Huang and Z. Li, *Anal. Chem.*, 2023, **95**, 11741–11750.
27 J. D. D. Habimana, R. Huang, B. Muhoza, Y. N. Kalisa, X. Han, W. Deng and Z. Li, *Biosens. Bioelectron.*, 2022, **203**, 114033.
28 M. Sohail, S. Xie, X. Zhang and B. Li, *Anal. Chim. Acta*, 2022, **1205**, 339541.
29 C. Wu, Z. Chen, C. Li, Y. Hao, Y. Tang, Y. Yuan, L. Chai, T. Fan, J. Yu, X. Ma, O. A. Al-Hartomy, S. Wageh, A. G. Al-Sehemi, Z. Luo, Y. He, J. Li, Z. Xie and H. Zhang, *Nano-Micro Lett.*, 2022, **14**, 159.
30 Z. Yi, J. De Dieu Habimana, O. Mukama, Z. Li, N. Odiwuor, H. Jing, C. Nie, M. Hu, Z. Lin, H. Wei and L. Zeng, *Biosensors*, 2021, **12**, 11.
31 M. J. Kellner, J. G. Koob, J. S. Gootenberg, O. O. Abudayyeh and F. Zhang, *Nat. Protoc.*, 2019, **14**, 2986–3012.
32 J. Shen, Z. Chen, R. Xie, J. Li, C. Liu, Y. He, X. Ma, H. Yang and Z. Xie, *Biosens. Bioelectron.*, 2023, **237**, 115523.
33 T. J. Xie, J. L. Xie, Y. J. Luo, K. Mao, C. Z. Huang, Y. F. Li and S. J. Zhen, *Anal. Chem.*, 2023, **95**, 7237–7243.
34 A. Imbriano, A. Tricase, E. Macchia, L. Torsi and P. Bollella, *Anal. Chim. Acta*, 2023, **1252**, 341037.
35 M. Nishita, S.-Y. Park, T. Nishio, K. Kamizaki, Z. Wang, K. Tamada, T. Takumi, R. Hashimoto, H. Otani, G. J. Pazour, V. W. Hsu and Y. Minami, *Sci. Rep.*, 2017, **7**, 1.
36 X. Wang, X. Lou, Y. Wang, Q. Guo, Z. Fang, X. Zhong, H. Mao, Q. Jin, L. Wu and H. Zhao, *Biosens. Bioelectron.*, 2010, **25**, 1934–1940.
37 A. Washizaki, A. Murayama, M. Murata, T. Kiyohara, K. Yato, N. Yamada, H. H. Aly, T. Tanaka, K. Moriishi, H. Nishitsuji, K. Shimotohno, Y. Goh, K. J. Ishii, H. Yotsuyanagi, M. Muramatsu, K. Ishii, Y. Takahashi, R. Suzuki, H. Akari and T. Kato, *Nat. Commun.*, 2022, **13**, 5207.
38 N. D. Marino, R. Pinilla-Redondo and J. Bondy-Denomy, *Nucleic Acids Res.*, 2022, **50**, 6414–6422.

 This journal is © The Royal Society of Chemistry 2025